Hydrogen transfer in photo-excited phenol/ammonia clusters by UV–IR–UV ion dip spectroscopy and *ab initio* molecular orbital calculations. II. Vibrational transitions

Shun-ichi Ishiuchi
Department of Chemistry, Faculty of Science and Technology, Keio University, 3-12-1 Hiyoshi, Kohoku-ku, Yokohama 223-8522, Japan and Institute for Molecular Science, 444-8585 Okazaki, Japan

Kota Daigoku
Computer Center and Department of Chemistry, Tokyo Metropolitan University/ACT-JST, 1-1 Minami-Ohsawa, Hachioji 192-0397, Japan

Morihisa Saeki and Makoto Sakai
Institute for Molecular Science, 444-8585 Okazaki, Japan

Kenro Hashimoto[a)]
Computer Center and Department of Chemistry, Tokyo Metropolitan University/ACT-JST, 1-1 Minami-Ohsawa, Hachioji 192-0397, Japan

Masaaki Fujii[b)]
Institute for Molecular Science, 444-8585 Okazaki, Japan

(Received 2 July 2002; accepted 30 July 2002)

The vibrational spectra of phenol/ammonia clusters (1:2–5) in S_0 and those of their photochemical reaction products, $(NH_3)_{n-1}NH_4$ $(n=2-5)$, which are generated by excited-state hydrogen transfer, have been measured by UV–IR–UV ion dip spectroscopy. The geometries, IR spectra and normal modes of phenol-$(NH_3)_n$ $(n=1-5)$ have been examined by *ab initio* molecular orbital calculations, at the second-order Møller–Plesset perturbation theory level with large basis sets. For the $n=2$ and 3 reaction products, similar vibrational analyses have been carried out. From the geometrical information of reactants and products, it has been suggested that the reaction products have memories of the reactant's structure, which we call "*memory effect*." © *2002 American Institute of Physics.* [DOI: 10.1063/1.1508104]

I. INTRODUCTION

It is well known that the acidic nature of the phenolic OH group increases when the aromatic ring is electronically excited to S_1. Phenol, naphthol and their derivatives embedded in ammonia clusters, which are typical acid-base pair complexes, have been investigated as a model system in order to study excited-state proton transfer (ESPT) for a long time.[1–18] Recently, phenol/ammonia clusters, PhOH–$(NH_3)_n$, have attracted renewed attention since Jouvet and co-workers proposed that not proton transfer, but hydrogen transfer (ESHT), occurs in S_1.[19–22]

In Paper I, we reported on the electronic spectra of the reaction products. By comparing them with the electronic spectra of $(NH_3)_{n-1}NH_4$ generated by the photolysis of pure ammonia clusters, we proved that the reaction products are the $(NH_3)_{n-1}NH_4$ produced by the ESHT. In addition, a theoretical analysis of the spectra indicated that the reaction products contain some isomers, at least for $n=3$ and 4. Though the electronic spectrum well reflects the molecular species and its electronic structures, the reaction mechanism, including the isomerization processes, remains unresolved.

To understand the reaction mechanism, the geometrical information at the initial and final stages of the reaction is indispensable. One of the best methods to obtain such information is vibrational spectroscopy, because NH vibrations are expected to sensitively reflect the hydrogen-bond network, in other words, the solvation structures in both the reactant and the product.

In this work, we measured the IR spectra of PhOH–$(NH_3)_n$ $(n=2-5)$ and the reaction products of the ESHT, i.e., $(NH_3)_{n-1}NH_4$ $(n=2-5)$ by UV–IR–UV ion dip spectroscopy. We also carried out *ab initio* molecular orbital (MO) calculations at the correlated level on the structures and the vibrational transitions of the reactants and products, and analyzed the experimental IR spectra. Based on the optimized geometries, we discuss the reaction mechanism.

II. EXPERIMENT

Figure 1(a) shows the principle of UV–IR–UV ion dip spectroscopy used to measure the vibrational transition of the reaction products $(NH_3)_{n-1}NH_4$ via photoexcited PhOH–$(NH_3)_n$. The methodology is essentially the same as the UV-near-IR–UV ion dip spectroscopy for the electronic spectra of the reaction products reported in Paper I. Briefly, the pump UV laser (ν_{UV}) was tuned to the S_1-S_0 transition of PhOH–$(NH_3)_n$ $(n=2-5)$. After a long time delay (200 ns), the ionization laser (ν_{ION}) was irradiated. After 20 ns

a)Electronic mail: hashimoto-kenro@c.metro-u.ac.jp
b)Electronic mail: mfujii@ims.ac.jp

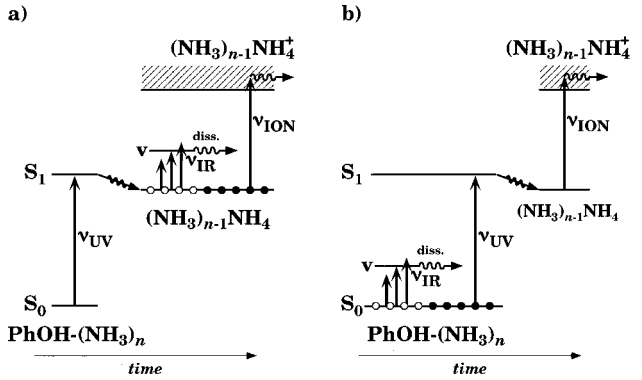

FIG. 1. Principle of the UV–IR–UV ion dip spectroscopy for (a) reaction products, $(NH_3)_{n-1}NH_4$, and (b) reactants, PhOH–$(NH_3)_n$ in the S_0 state.

from the υ_{UV}, the IR laser (υ_{IR}) was irradiated and scanned from 2660 to 3760 cm^{-1}. If υ_{IR} is resonant to a certain vibrational transition, the cluster is predissociated. As a result, the ion signal of $(NH_3)_{n-1}NH_4^+$ decreases. The vibrational transition of the $(NH_3)_{n-1}NH_4$ which generates $(NH_3)_{n-1}NH_4^+$ can be observed as a depletion of the ion signal. Similarly, the vibrational spectra of the PhOH–$(NH_3)_n$ in S_0 can be measured as an ion dip when the order of υ_{UV} and υ_{IR} is changed in time [see Fig. 1(b)].

The experimental setup was the same as that described in Paper I, except for the mid-IR laser generation. The IR laser was obtained by differential mixing between the output of a dye laser (Lumonics HD-500/DCM) pumped by the second harmonic of a YAG laser (Continuum Powerlite 8100) and 532 nm in a $LiNbO_3$ crystal. The typical power of υ_{IR} was 0.2 mJ.

III. COMPUTATIONAL METHOD

Molecular structures of PhOH–$(NH_3)_n$ ($n=1-5$) were optimized by using the energy gradient technique at the MP2/6-31++G(d,p) level with the usual frozen core approximation. Vibrational analyses were carried out at each optimized geometry to confirm the minima on the potential energy surfaces. The second derivative matrices for $n \leqslant 3$ were computed analytically, while those for $n \geqslant 4$ were obtained by numerically differentiating the first derivatives along the nuclear coordinates. The IR intensities of each vibration were evaluated for all minimum structures. The total binding energies, including a zero-point vibrational correction (ZPC), were computed by using scaled harmonic frequencies. The scale factor (0.941) was determined by the average ratio between the experimental fundamental[23] and the calculated harmonic frequencies of the symmetric NH stretch (υ_1) of a PhOH–$(NH_3)_1$ cluster. The basis set superposition errors for the total binding energies were corrected by a counterpoise correction (CPC). We used the GAUSSIAN 98 program.[24]

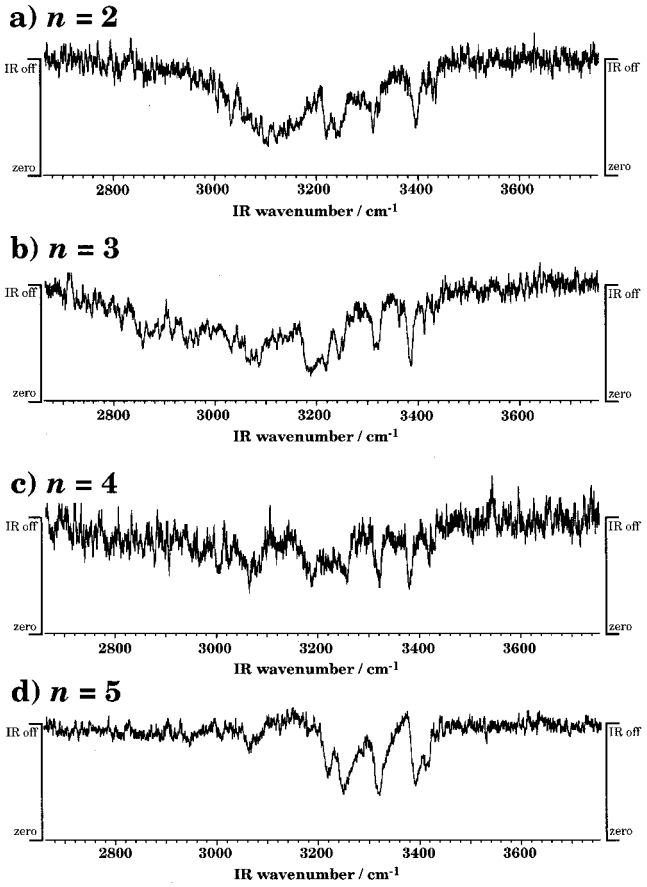

FIG. 2. UV–IR–UV ion dip spectra of PhOH–$(NH_3)_n$ in S_0 state. The pump laser υ_{UV} was fixed to (a) $n=2$: 35 544 cm^{-1}, (b) $n=3$: 35 498 cm^{-1}, (c) $n=4$: 35 348 cm^{-1}, and (d) $n=5$: 282.5 nm, respectively. The ionization laser υ_{ION} was fixed to 306.5 nm for the $n=2$, and for the other sizes ($n=3-5$), 355 nm was used.

IV. RESULTS AND DISCUSSION

A. Reactants, PhOH–$(NH_3)_n$ in S_0

1. UV–IR–UV ion dip spectra for n=2–5

Figure 2 shows the vibrational spectra of the reactants PhOH–$(NH_3)_n$ ($n=2-5$) in S_0. The spectra for $n=3$ and 4, reported previously,[25] are also included for a comparison.

The IR dip spectrum of PhOH–$(NH_3)_2$ has been partially reported by Schmitt *et al.*[18] They labeled the population of the cluster by one-color REMPI, while we monitored the population in S_0 by two-color ionization. The present spectrum for the $n=2$ spectrum in Fig. 2(a) corresponds well to theirs. Some sharp bands at 3200–3500 cm^{-1} on the very broad background centered at about 3100 cm^{-1} were observed.

Figures 2(b) and 2(c) show vibrational spectra of PhOH–$(NH_3)_3$ and PhOH–$(NH_3)_4$. The pump laser υ_{UV} was fixed to 35 498 cm^{-1} ($n=3$) and 35 348 cm^{-1} ($n=4$), respectively. The ionization laser υ_{ION} was fixed to 355 nm for both sizes. In both spectra, some sharp bands at 3200–3400 cm^{-1} are observed on a very broad background signal, which well resembles the spectrum of PhOH–$(NH_3)_2$. From the similarity, the sharp bands at 3200–3400 cm^{-1} and the broad background are tentatively assigned to the NH stretch vibrations and the OH stretch vibration, respectively. Some

weak peaks at 3100 cm^{-1} are assigned to CH stretch vibrations. The OH stretch bands are much broader than that of $n=2$. Detailed assignments are discussed later.

Shown in Fig. 2(d) is a spectrum of $PhOH-(NH_3)_5$ obtained by fixing υ_{UV} and υ_{ION} to the center of the broad peak (282.5 nm) and 355 nm, respectively. Sharp peaks which can be assigned to CH stretch and NH stretch vibrations are observed at 3060 and 3200–3440 cm^{-1} without a broad background. For $PhOH-(NH_3)_n$ clusters in the S_0 state, the smallest size with which the proton transfer occurs has been reported to be 6.[26] Since $n=5$ is the limit size of non proton transferred species in S_0 the OH bond in $PhOH-(NH_3)_5$ is expected to be lengthened due to the strong hydrogen bonds. The OH stretch band may be extremely broadened and/or shifted down to a lower frequency region than that scanned by us.

2. Optimized geometries and energetic for n=0–5

The optimized geometries and total binding energies (TBEs) of $PhOH-(NH_3)_n$ $(n=0-5)$ at the MP2/6-31++G(d,p) level are shown in Fig. 3. The TBE values given in the following text are with both ZPC and CPC.

In the 1:1 complex, **Ia**, PhOH denotes an OH bond to hydrogen-bonding with NH_3. Its TBE is -6.0 kcal/mol. Two $n=2$ clusters, **IIa** and **IIb**, are almost isoenergetic; their TBEs are -10.6 kcal/mol. The second NH_3 is bound to a NH_3 site in **Ia** with pointing an NH bond to oxygen of PhOH (**IIa**) or to a π electron cloud (**IIb**). These structures are essentially the same as that of the cyclic and open isomers reported by Schmitt *et al.*[18] Four $n=3$ structures were optimized. Two cyclic structures, **IIIa** and **IIIb**, are the most stable and their TBEs are around -15 kcal/mol. They have a very similar hydrogen-bond network with only a slightly different internal rotation angle of OH about the O–C bond. In **IIIc** and **IIId**, the third NH_3 is hydrogen bonded to an NH_3 in **IIa**. The optimization starting from the structure where the third ammonia is bound to the NH_3, labeled α in **IIb**, also converged to **IIId**. These two structures are less stable than **IIIa** by $\sim$1–2 kcal/mol. Five $n=4$ structures were examined. **IVa** is a cyclic structure, while **IVb** and **IVd** are isomers with the fourth NH_3 bound to a free NH in **IIIb** and **IIIc**, respectively. **IVc** has a four-membered hydrogen-bonded ring with an NH_3 located outside the ring. It can also be regarded as a structure where an NH_3 molecule is inserted to the cyclic hydrogen bonds in **IIIc**. These four structures are as stable as one another, and their TBEs range from -18.1 to -16.6 kcal/mol. On the other hand, the OH bond is broken in **IVe**. It is found by the electron distribution that this is an ion-pair structure where the $NH_4^+(NH_3)_3$ is bound to PhO^- by pointing the NH in each solvent NH_3 to oxygen. The TBE of **IVe** is -7.7 kcal/mol, which is about 10 kcal/mol less than those of other isomers where the OH bond remains. Since the number of minimum-energy configurations is expected to be very large for $n=5$, we have concentrated on five structures for this size. **Va** is a cyclic form, whose TBE is -20.4 kcal/mol. **Vb** and **Vc** can be regarded as structures in which the fifth solvent molecule bridges two ammonia molecules in **IVa** and **IVb**, respectively. Their TBEs are about -21 kcal/mol. **Vd** and **Ve** are ion-pair isomers where a solvated NH_4^+ is bound to PhO^-. The NH_4^+ is bound directly to the counter ion by a single NH bond in the former, while the two ions with opposite charges are bridged by three solvents in the latter. The TBEs of **Vd** and **Ve** are -20.3 and -16.4 kcal/mol, respectively.

Siebrand *et al.* have reported the cyclic structures of $PhOH-(NH_3)_{2,3}$ calculated at the BLYP/6-31G(d) level.[27] They also optimized $PhOH-(NH_3)_{4,5}$, in which the fourth and fifth NH_3 molecules are hydrogen bonded to free NH bond(s) in the NH_3 accepting OH in the cyclic $PhOH-(NH_3)_3$ at the BLYP/6-31G(d) $(n=4)$ and HF/6-31G(d) $(n=5)$ levels. No ion-pair structure was found by their calculations for $n\leqslant 4$, while the ionic isomer for $n=5$ was less stable than the nonionic form by $\sim$6 kcal/mol. The present calculations show that the ion-pair complex is much less stable than the cyclic one for $n=4$. The proton transferred (PT) clusters become very close in energy to the most stable form, but they are not yet the most stable for $n=5$ even at the MP2/6-31++G(d,p) level.

3. Band assignments and cluster structures responsible for experimental spectra

The calculated harmonic frequencies, IR intensities and normal modes of $PhOH-(NH_3)_n$ $(n=0-3)$ and a free NH_3 are listed in Table I. We use the symbolic letters α, β, γ,..., to denote each NH_3 molecule in the clusters in the following paragraphs and tables. They correspond to the labels of NH_3 in each structure in Fig. 3.

The IR spectrum of the 1:1 complex has been reported by Iwasaki *et al.* and the intense band at 3294 cm^{-1} and a weak band at 3333 cm^{-1} have been assigned to the OH stretch and the asymmetric NH stretch, respectively.[23] They also assigned two other weak bands at 3058 and 3088 cm^{-1} to a CH stretch.

As mentioned above, the UV–IR–UV ion dip spectrum for $PhOH-(NH_3)_2$ is similar to the IR–R2PI spectrum reported by Schmitt *et al.*[18] They have assigned all five bands observed in the region higher than 3200 cm^{-1} to symmetric and asymmetric NH stretch vibrations based on calculations at the MP2/6-31G(d) level, though they could not definitely determine the cluster geometry. We are also unable to argue about the cyclic and open arrangements of the $(NH_3)_2$ group, because these structures show nearly identical frequencies and intensities, even at the present level of calculation. However, a comparison between the present experimental and theoretical results together with $n=1$ and 3 clusters offers alternative assignments for $n=2$.

The observed and calculated spectra for $n=2$ and 3 together with the theoretical result for $n=1$ are shown in Fig. 4. The spectrum of **IIb** is not shown for brevity. The theoretical spectrum of **IIIb** is also excluded because it is almost the same as that of **IIIa**; we cannot determine the internal rotation angle of OH for $n=3$.

We see in the lower part of the figure that the observed spectrum for $n=3$ is better reproduced by **IIIa** than **IIIc** and **IIId** because the latter isomers have no strong band at around 3200 cm^{-1}. Thus, we can safely rule out **IIIc** and **IIId**. In the following paragraphs, we denote the vibrations

TABLE I. Harmonic frequencies (cm^{-1}) and IR intensities (km/mol) of CH, NH, and OH stretches in phenol-$(NH_3)_{0-3}$ clusters at MP2/6-31++G(d,p) level.

NH_3		phenol		phenol-$(NH_3)_1$			phenol-$(NH_3)_2$					phenol-$(NH_3)_3$									
					Ia			**IIA**		**IIb**			**IIIa**		**IIIb**		**IIIc**		**IIId**		
Expt.[a]	Calc.	Expt.[b]	Calc.	Expt.[c]	Calc.	Int.	Expt.	Calc.	Int.	Calc.	Int.	Expt.	Calc.	Int.	Calc.	Int.	Calc.	Int.	Calc.	Int.	Mode
		3657	3631	3294	3260	1165		3097	1339	3097	1215		2966	1522	2956	1680	2843	1700	2821	1873	OH str
			3043	3058	3050	5		3051	6	3050	6		3050	3	3050	3	3050	4	3049	4	CH str
			3060	3088	3058	5		3057	10	3058	11		3057	7	3057	10	3057	7	3057	10	CH str
			3069		3069	21		3068	0	3072	5		3071	16	3074	18	3071	16	3074	18	CH str
			3081		3077	19		3075	21	3075	13		3078	25	3080	14	3074	18	3079	15	CH str
			3087		3083	9		3082	77	3082	59		3083	5	3085	5	3082	7	3083	2	CH str
3337	3352			3333	3334	12	3239	3264	139	3259	177	3188	3204	283	3216	251	3260	77	3267	58	H-bonded NH str (α,υ_1)
							3311	3318	52			3243	3257	137	3244	191	3315	43	3317	11	H-bonded NH str (β,υ_1)
										3322	4										π-bonded NH str (β,υ_1)
												3313	3307	49	3311	25	3320	16	3321	10	H-bonded NH str (γ,υ_1)
					3479	15	3416	3429	65	3425	64	3363	3409	58	3411	65	3388	162	3412	153	H-bonded NH str (α,υ_3)
							3435	3462	68			3386	3414	55	3413	66	3461	62	3460	23	H-bonded NH str (β,υ_3)
										3464	6										π-bonded NH str (β,υ_3)
												3413	3451	56	3450	35	3465	40	3465	34	H-bonded NH str (γ,υ_3)
								3486	8	3475	10	3431	3471	6	3471	3	3488	5	3480	4	non-H-bonded NH str (β,υ_3)
3444	3512				3483	15		3485	11	3480	10		3475	9	3476	10	3469	30	3469	20	non-H-bonded NH str (α,υ_3)
													3481	4	3475	5	3479	8	3480	8	non-H-bonded NH str (γ,υ_3)

[a]Reference 28.
[b]Reference 29.
[c]Reference 23.

derived from symmetric NH stretch in NH_3 as υ_1, and those from asymmetric NH stretch as υ_3.

We now compare the spectra for **IIa** and **IIIa** with the experiment in detail. First of all, the OH stretch, whose calculated frequency is 3097 cm^{-1}, is the most intense for **IIa**, and the CH stretch frequencies in this cluster are computed to be ~3050–~3080 cm^{-1}. In the spectrum for **IIIa**, the OH stretch is also the strongest, being redshifted to ~2970 cm^{-1}, while the CH stretch bands do not change very much from those of **IIa**. Thus, the broad bands at around 3100 cm^{-1} in both the $n=2$ and 3 spectra are assignable to the overlapping between OH and CH stretch vibrations in **IIa** and **IIIa**, respectively. The remarkable red shifts of the OH stretch with increasing cluster size is similar to naphthol–$(H_2O)_n$, having the cyclic hydrogen-bond network.[30]

Second, if we look at a region higher than ~3350 cm^{-1}, two calculated bands in **IIa**, in which the υ_3 mode with the stretching of the hydrogen-bonded NH is a main contributor, correspond well to the observed bands at 3395 and 3435 cm^{-1}. Similarly, three υ_3 bands calculated for **IIIa** also well reproduce the observed bands at 3363, 3386, and 3413 cm^{-1}, while another observed band at 3431 cm^{-1} is assignable to the overlapping of three quasidegenerate υ_3 bands of free NH bonds. Thus, the bands in this region in the experimental spectra for $n=2$ and 3 can be assigned to asymmetric NH stretches in **IIa** and **IIIa**. It is interesting to note that the frequencies of non-hydrogen-bonded NH stretches in **IIIa** become close to the average of the υ_1 and υ_3 frequencies of a free NH_3, which indicates the localization of the NH stretch vibrations.

Third, in the region from ~3150 to ~3350 cm^{-1}, the calculated υ_1 bands due to two NH_3 molecules in **IIa** correspond well to the observed bands at ~3240 and ~3310 cm^{-1}, which are redshifted from $n=1$ by ~20 and ~90 cm^{-1}, respectively. The lower and higher bands can be assigned to the hydrogen-bonded NH stretch at α NH_3 and the υ_1 mode at β NH_3 in **IIa**, respectively. Three theoretical υ_1 bands in **IIIa** also well reproduce the positions and relative intensities of the observed bands in this region. Thus, the two low bands among them are assignable to the hydrogen-bonded NH stretch at the α and β NH_3 molecules, respectively. They are redshifted nearly in parallel with each other from $n=2$. The ~3310 cm^{-1} band is considered to be the υ_1 mode in γ NH_3. This band is only slightly redshifted from the corresponding bands in $n=1$ and 2 because of the week interaction between O and NH in the terminal NH_3.

On the other hand, the presence of the band at ~3220 cm^{-1} in the observed spectra for both $n=2$ and 3 seems to contradict with the number of υ_1 bands expected for the clusters. Schmitt *et al.* assigned two bands at 3219 and 3239 cm^{-1} in their spectrum to the symmetric NH stretches, two at 3311 and 3395 cm^{-1} to the symmetric stretches of bound NH and the rest at 3435 cm^{-1} to the same mode of free NH bonds.[18] However, it is worth reminding that we can expect the overtone of the υ_4 vibration (the degenerate bending of NH_3) near this frequency. In fact, the υ_4 frequencies are calculated to be 1590–1640 cm^{-1} for both **IIa** and **IIIa**. Thus, the ~3220 cm^{-1} band may be due to the overtone of the υ_4 vibrations because they are almost size independent for $n=2$ and 3. It is also because the theoretical results for $n=1-3$ all together well explain the frequencies of the υ_1 and υ_3 bands and their systematic shifts with increasing n in relation to the positions of NH_3 molecules in the hydrogen-bond network in **IIa** and **IIIa**.

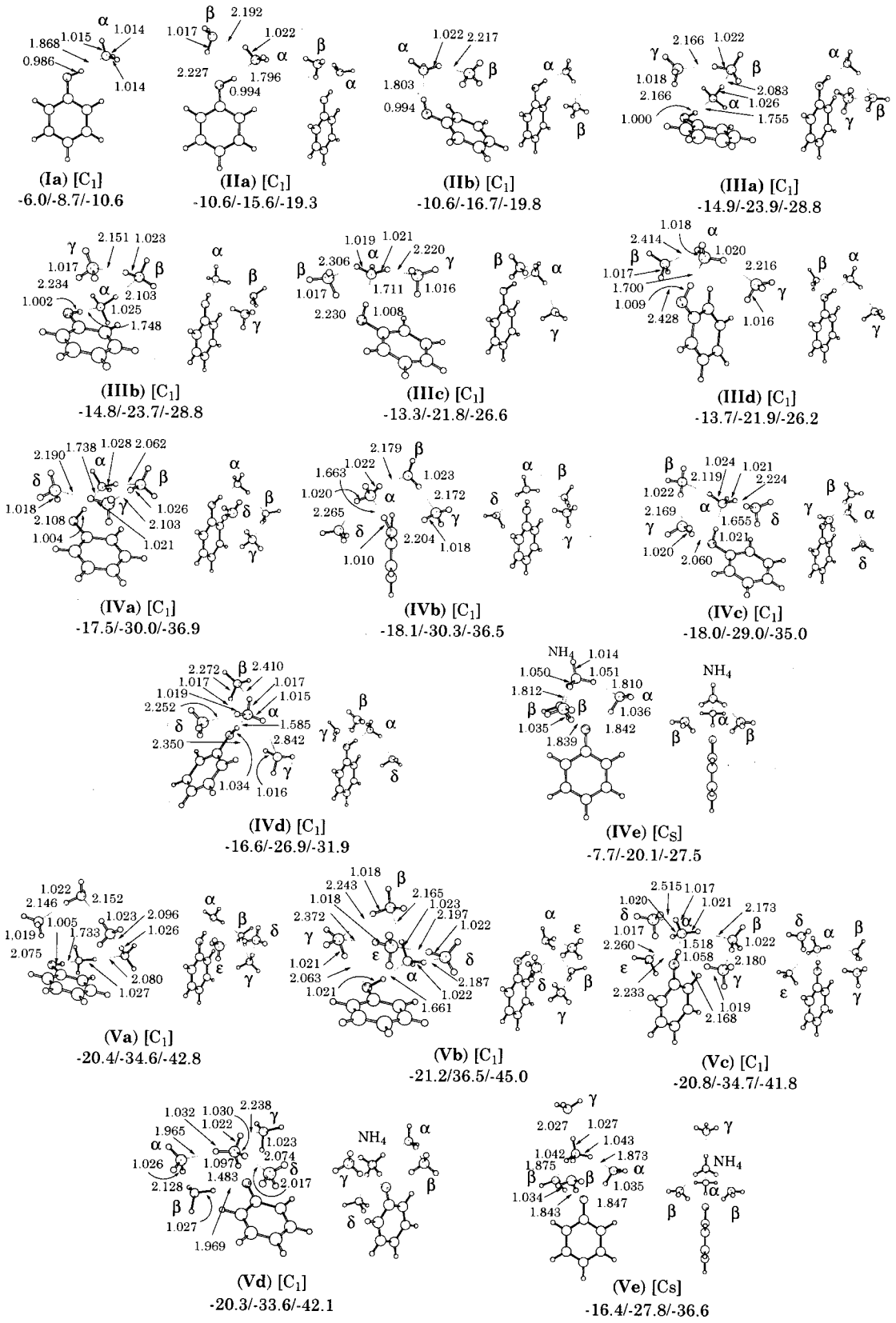

FIG. 3. Optimized geometries of PhOH–$(NH_3)_n$ ($n=1-5$) in S_0 state at the MP2/6-31++G(d,p) level. Molecular symmetry and total binding energies (TBEs) (kcal/mol) are presented. Values of TBEs are with ZPC and CPC (left), without CPC (center), and without ZPC and CPC (right). Geometrical parameters are given in Å and degrees.

The observed and calculated spectra for $n=4$ and 5 are compared in Figs. 5 and 6. The calculated harmonic frequencies, IR intensities and normal modes for PhOH–$(NH_3)_{4,5}$ are listed in Tables II and III.

The observed spectrum for $n=4$ is best reproduced by **IVa** having the cyclic hydrogen bonds. The CH and OH stretches are calculated at ~3050–~3090 cm^{-1} and 2913 cm^{-1}, respectively; the band at ~3070 cm^{-1} and its broad

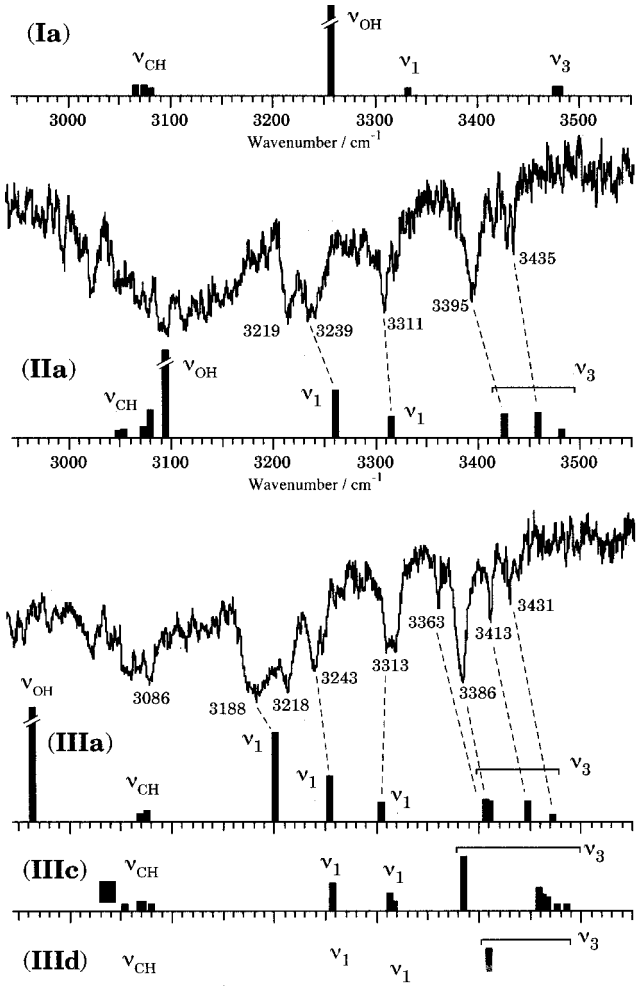

FIG. 4. Theoretical IR spectra of PhOH–$(NH_3)_n$ ($n=1-3$) compared with the experimental ones ($n=2$ and 3). Each theoretical spectrum (**Ia**), (**IIa**),..., belongs to each optimized geometry shown in Fig. 3.

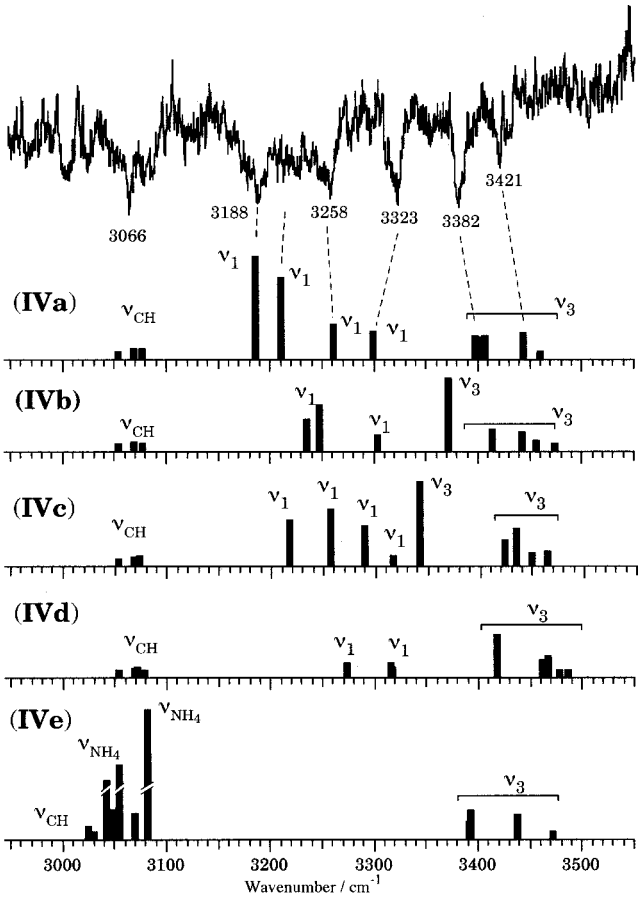

FIG. 5. Theoretical IR spectra of PhOH–$(NH_3)_4$ compared with the experimental one. Each theoretical spectrum (**IVa**), (**IVb**),..., belongs to each optimized geometry shown in Fig. 3.

background can be assigned to these stretch vibrations. We can ascribe the bands observed at 3382 and 3421 cm^{-1} to non-hydrogen-bonded NH stretches, while three strong bands at 3188, 3258, and 3323 cm^{-1} to the hydrogen-bonded NH stretches. The calculations suggest that the weak band at $\sim$3220 cm^{-1} is also probably due to the same mode at β NH_3, though the overtone of υ_4 in solvents may overlap, as was the case for $n=2$ and 3. The position of the lowest band in the hydrogen-bonded NH stretch region for $n=4$ does not change very much from $n=3$ in both experiment and theory. This reduced redshift compared to that for $n=2\rightarrow3$ is consistent with only a small lengthening of the hydrogen-bonded NH bond in α NH_3. It is elongated by 0.004 Å from $n=2$ to 3 and by 0.002 Å from $n=3$ to 4.

For $n=5$, only three bands are observed in the υ_1 region, but have the following characteristics: (i) the lowest υ_1 band is slightly blueshifted from $n=4$, in contrast to the smaller clusters, (ii) this lowest υ_1 band is located at the same position as the υ_4 overtone bands for $n\leqslant4$, (iii) two higher bands are broad compared to $n\leqslant4$, suggesting that the overlapped transitions and their peaks are separated by $\sim$70 cm^{-1}. We now examine the theoretical spectra for $n=5$ isomers with respect to these features.

At first, there is only one strong band in this region for **Ve**. **Vd** has the second strongest band at 3171 cm^{-1}, being redshifted from the 3189 cm^{-1} band for **IVa**, while the most intense band for **Va** does not move from the corresponding band for **IVa**. Therefore, the proton transferred (ion pair) and cyclic complexes should be expelled.

Two calculated υ_1 frequencies (3303 and 3297 cm^{-1}) are almost degenerate for **Vb**. Four bands with nearly equal intensities and spacings are expected in the υ_1 region for this complex, which differs from the experimental observation. We thus exclude **Vb**. The strong υ_3 band shifted down to 3339 cm^{-1} also supports this conclusion.

On the other hand, five υ_1 bands for **Vc** are calculated at 3240, 3255, 3301, 3318, and 3320 cm^{-1}, with the two highest ones being nearly degenerate. The frequency difference between the two lower bands and that among the other three are only 15 and 19 cm^{-1}, respectively, while these two groups are separated by $\sim$60 cm^{-1}. It is plausible that the overlapping of the two lower bands corresponds to the observed 3246 cm^{-1} band and that of the three higher ones to the 3319 cm^{-1} band. The lowest υ_1 bands in this complex are blueshifted from $n=4$, which is coherent with the shortenings of the bonded NH in α NH_3. In addition, the calculated υ_4 frequencies for **Vc** (1589–1641 cm^{-1}) are almost unchanged from $n=2$ and 3, which is consistent with the presence of the 3221 cm^{-1} band. For this complex, a rela-

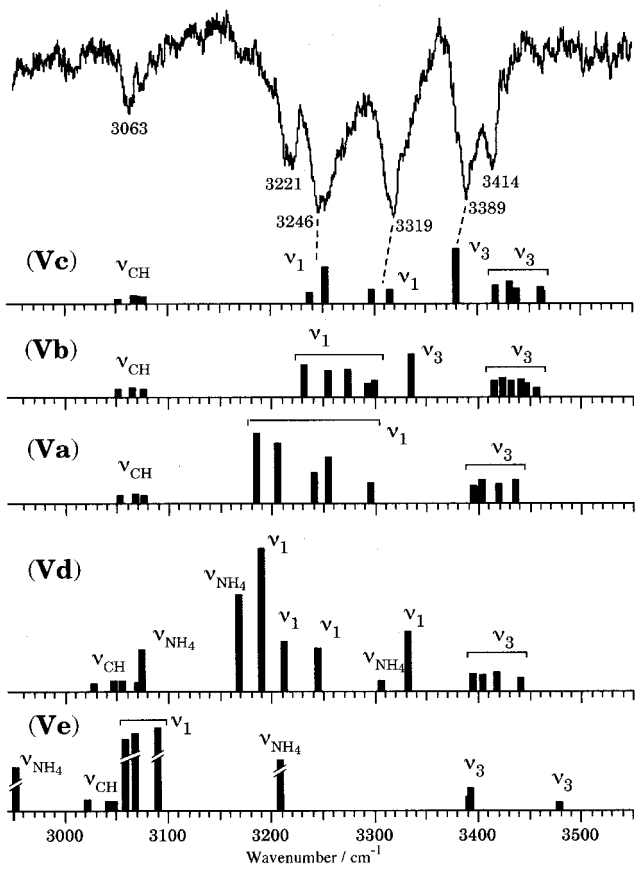

FIG. 6. Theoretical IR spectra of PhOH–$(NH_3)_5$ compared with the experimental one. Each theoretical spectrum (**Vc**), (**Vb**),..., belongs to each optimized geometry shown in Fig. 3.

tively intense band and five weak bands derived from the hydrogen-bonded NH stretches are calculated to be at 3382 and 3420–3466 cm^{-1}, respectively. The observed broad band with two peaks at 3389 and 3414 cm^{-1} can be attributed to an overlapping of these transitions. The CH stretch frequencies for **Vc** are calculated at 3048–3080 cm^{-1}, which correspond well to the observed band at ~3060 cm^{-1}. Note that the OH stretch frequency of this cluster is calculated to be 2019 cm^{-1}, being extremely lowered from $n=4$. The large redshift of this band down to a region lower than that examined by the experiment is consistent with the disappearance of the broad background at around 3000 cm^{-1}. Therefore, the observed spectrum for $n=5$ is considered to stem from **Vc**. The OH bond is elongated by more than 0.07 Å from a bare PhOH, but the hydrogen is still located at the oxygen site.

In summary, based on a comparison between the experimental and theoretical spectra, those clusters, in which $(NH_3)_n$ solvate PhOH in the chainlike structure with one terminal NH_3 bound to OH, are considered to be responsible for the experimental spectra for $n=2-4$. The cyclic hydrogen-bond network including OH is formed for $n=3$ and 4. On the other hand, in the $n=5$ cluster, which well reproduces the observed spectral features, all of the three NH bonds in NH_3 bound directly to (O)H by a nitrogen lone pair are used in the hydrogen-bond network with other solvents. It is interesting to note that the structure of the $(O)H\cdots(NH_3)_5$ part in the cluster resembles the second most stable form of$(NH_3)_4NH_4$, rather than the most stable one found by theoretical calculations in Paper I.

TABLE II. Harmonic frequencies (cm^{-1}) and IR intensities (km/mol) of CH, NH and OH stretches in phenol-$(NH_3)_4$ clusters at MP2/6-31++G(d,p) level.

	phenol-$(NH_3)_4$											
	IVa		**IVb**		**IVc**		**IVd**			**IVe**		
Expt.	Calc.	Int.	Calc.	Int.	Calc.	Int.	Calc.	Int.	Mode	Calc.	Int.	Mode
	2913	1761	2667	2058	2625	2196	2395	2497	OH str	2792	845	H-bonded NH str (NH_4,υ_3) (A')
	3047	3	3048	3	3050	4	3049	4	CH str	2803	779	H-bonded NH str (NH_4,υ_1) (A')
	3057	6	3056	12	3057	7	3056	8	CH str	2806	944	H-bonded NH str (NH_4,υ_3) (A'')
	3071	19	3072	16	3071	18	3071	14	CH str	3026	28	CH str (A')
	3079	16	3079	11	3076	20	3074	15	CH str	3032	10	CH str (A')
	3089	4	3087	1	3082	5	3081	9	CH str	3044	758	H-bonded NH str (α,υ_1) (A')
3188	3189	337	3238	91	3221	139	3276	30	H-bonded NH str (α,υ_1)	3045	8	CH str (A')
	3213	262	3250	141	3260	178	3318	34	H-bonded NH str (β,υ_1)	3051	91	CH str (A')
3258	3263	101	3306	40	3292	118	3320	18	H-bonded NH str (γ,υ_1)	3056	810	H-bonded NH str (β,υ_1) (A'')
3323	3302	78			3320	19			H-bonded NH str (δ,υ_1)	3071	74	CH str (A')
			3322	2			3320	13	π-bonded NH str (δ,υ_1)	3084	999	H-bonded NH str (α,β,υ_1) (A')
3382	3400	63	3416	61	3426	74	3464	43	H-bonded NH str (β,υ_3)	3393	36	non-H-bonded NH str (α,υ_3) (A'')
	3403	55	3374	238	3344	265	3420	132	H-bonded NH str (α,υ_3)	3393	42	non-H-bonded NH str (β,υ_3) (A'')
	3410	59	3445	49	3438	110	3465	23	H-bonded NH str (γ,υ_3)	3395	81	non-H-bonded NH str (β,υ_3) (A')
3421	3447	71							H-bonded NH str (δ,υ_3)	3440	70	non-H-bonded NH str (NH_4,υ_3) (A')
			3467	5	3467	34	3465	42	π-bonded NH str (δ,υ_3)	3473	3	non-H-bonded NH str (β,υ_3) (A'')
	3463	9	3475	4	3479	5	3483	3	non-H-bonded NH str (γ,υ_3)	3473	12	non-H-bonded NH str (β,υ_3) (A')
	3466	3	3472	3	3482	4	3488	5	non-H-bonded NH str (β,υ_3)	3474	8	non-H-bonded NH str (α,υ_3) (A'')
	3472	9	3458	22	3453	28			non-H-bonded NH str (α,υ_3)			
							3469	58	H-bonded NH str (α,υ_3)			
	3482	4	3476	8	3479	6	3481	7	non-H-bonded NH str (δ,υ_3)			

TABLE III. Harmonic frequencies (cm^{-1}) and IR intensities (km/mol) of CH, NH, and OH stretches in phenol-$(NH_3)_5$ clusters at MP2/6-31++G(d,p) level.

phenol-$(NH_3)_5$											
Vc		**Vb**		**Va**		**Vd**			**Ve**		
Calc.	Int.	Calc.	Int.	Calc.	Int.	Calc.	Int.	Mode	Calc.	Int.	Mode
2019	2919	2624	2205	2899	1806			OH str	2923	561	H-bonded NH str (NH_4,υ_1) (A')
						2089	2118	H-bonded NH str (NH_4,$\upsilon_3(\upsilon_{OH})$)	2945	414	H-bonded NH str (NH_4,υ_3) (A')
3048	4	3049	4	3050	2	3031	13	CH str	2954	446	H-bonded NH str (NH_4,υ_3) (A'')
3055	9	3055	10	3057	11	3039	4	CH str	3024	28	CH str (A')
3070	15	3069	18	3071	18	3049	26	CH str	3031	9	CH str (A')
3073	13	3079	14	3080	12	3058	26	CH str	3044	23	CH str (A')
3080	10	3094	3	3091	1	3073	20	CH str	3050	24	CH str (A')
						3077	184	H-bonded NH str (NH_4,υ_1)	3060	977	H-bonded NH str (α,υ_1) (A')
						3171	457	H-bonded NH str (NH_4,υ_3)	3070	1002	H-bonded NH str (β,υ_1) (A'')
3240	31	3235	128					H-bonded NH str (α,υ_1)	3070	51	CH str (A')
3255	158							H-bonded NH str (β,υ_1)	3092	1033	non-H-bonded NH str (α,υ_1) (A')
				3188	327	3193	692	in-phase H-bonded NH str (α,β,υ_1)	3211	871	H-bonded NH str (NH_4,υ_3) (A')
				3209	272	3214	228	out-of-phase H-bonded NH str (α,β,υ_1)	3334	1	non-H-bonded NH str (γ,υ_1) (A')
3301	47	3277	108			3247	190	H-bonded NH str (γ,υ_1)	3393	33	non-H-bonded NH str (α,υ_3) (A')
3318	43	3258	100					H-bonded NH str (δ,υ_1)	3393	39	non-H-bonded NH str (β,υ_3) (A'')
						3309	29	π-bonded NH str (δ,υ_1)	3395	84	non-H-bonded NH str (β,υ_3) (A')
				3244	127			in-phase H-bonded NH str (γ,δ,υ_1)	3472	2	non-H-bonded NH str (β,υ_3) (A'')
				3258	204			out-of-phase H-bonded NH str (γ,δ,υ_1)	3473	9	non-H-bonded NH str (β,υ_3) (A')
3320	10							π-bonded NH str (ε,υ_1)	3474	6	non-H-bonded NH str (α,υ_3) (A'')
				3299	75			H-bonded NH str (ε,υ_1)	3480	13	non-H-bonded NH str (γ,υ_3) (A'')
		3297	40					out-of-phase H-bonded NH str (β,ε,υ_1)	3480	13	non-H-bonded NH str (γ,υ_3) (A')
		3303	55					in-phase H-bonded NH str (β,ε,υ_1)			
						3335	274	H-bonded NH str (NH_4,υ_3)			
				3399	64			in-phase H-bonded NH str (α,β,υ_3)			
				3401	52			out-of-phase H-bonded NH str (α,β,υ_3)			
3382	251	3339	189			3407	56	H-bonded NH str (α,υ_3)			
3420	62	3445	61			3397	63	H-bonded NH str (β,υ_3)			
3434	90							H-bonded NH str (α,υ_3)			
		3450	37	3470	9	3473	6	non-H-bonded NH str (α,υ_3)			
3441	52	3427	70			3420	74	H-bonded NH str (γ,υ_3)			
				3407	90			π,H-bonded NH str (γ,υ_3)			
3464	58	3419	55	3423	73			H-bonded NH str (δ,υ_3)			
						3444	43	π-bonded NH str (δ,υ_3)			
3466	39							π-bonded NH str (ε,υ_3)			
		3435	52	3440	89			H-bonded NH str (ε,υ_3)			
3474	3	3470	4			3479	5	non-H-bonded NH str (γ,υ_3)			
				3465	11			π,non-bonded NH str (γ,υ_3)			
3475	4	3482	6	3466	3	3465	3	non-H-bonded NH str (β,υ_3)			
3481	7	3460	16	3478	4			non-H-bonded NH str (ε,υ_3)			
3488	4	3472	1	3479	3	3471	8	non-H-bonded NH str (δ,υ_3)			

B. Reaction products $(NH_3)_{n-1}NH_4$ ($n=2-5$)

1. UV–IR–UV ion dip spectra of the reaction products, $(NH_3)_{n-1}NH_4$ ($n=2-5$)

Figure 7 shows vibrational spectra of the reaction products $(NH_3)_{n-1}NH_4$ ($n=2-5$) generated via photoexcited PhOH–$(NH_3)_n$. The energies of the υ_{UV} and υ_{ION} lasers were the same as in the case of the measurement of the vibrational spectra of the PhOH–$(NH_3)_n$ in S_0. The spectra of $(NH_3)_{2,3}NH_4$ reported previously[25] are also included for a comparison.

As can be seen in Fig. 7(a), weak bands were observed at 3200–3300 cm^{-1} for NH_3NH_4, which is different from $NH_3NH_4^+$: An asymmetric NH stretch of NH_3 is observed at 3397.4 cm^{-1} for the cation.[31]

In the spectrum of the $n=3$ reaction product [Fig. 7(b)], we can see two intense bands at ~3180 and ~3250 cm^{-1} and a broad band in the region of 2700–3100 cm^{-1}. No band is observed in a region higher than 3300 cm^{-1}. This spectrum is remarkably different from that of $(NH_3)_2NH_4^+$, in which free NH stretching vibrations of NH_4^+ and NH_3 sites are observed at 3395.4 and 3413.7 cm^{-1}, respectively, without a broad band in the lower region.[31] As mentioned in Paper I, the $n=3$ spectrum contains the transitions from two isomers, though we cannot distinguish them by the present experiment. We recently measured the picosecond time-resolved IR spectrum and found that the ~3180 cm^{-1} band rises faster than the ~3250 cm^{-1} band.[32] This means that each band is derived from different species.

Similarly, two intense bands at ~3180 and at ~3240 cm^{-1} on some structured broad bands are observed for $(NH_3)_3NH_4$ [Fig. 7(c)]. As in the case of $n=3$, a very broad band below 3100 cm^{-1} is observed, but it does not extend to ~2600 cm^{-1}. As mentioned in Paper I, the very broad electronic absorption observed in $n=4$ suggests the coexistence

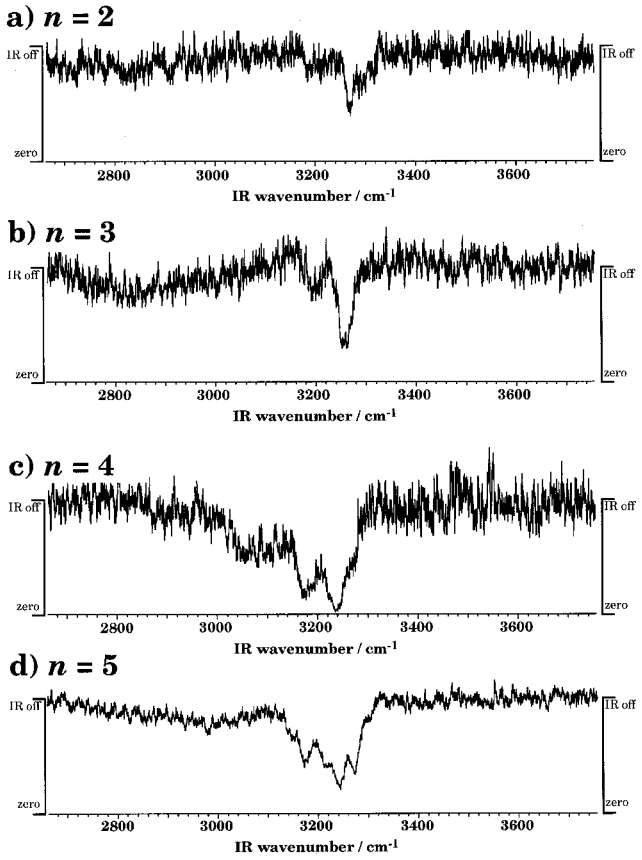

FIG. 7. UV–IR–UV ion dip spectra of $(NH_3)_{n-1}NH_4$. The conditions of v_{UV} and v_{ION} were the same as the case of PhOH–$(NH_3)_n$ (see Fig. 2 caption).

of some isomers. Thus, this spectrum is also expected to contain the vibrational transitions of some isomers.

We can see five peaks at 3140, 3171, 3211, 3243, and 3273 cm^{-1} in the spectrum of the reaction product $(NH_3)_4NH_4$ [Fig. 7(d)], which are narrower than those in smaller products. A very broad band below 3100 cm^{-1} was also observed as in the case of $n=3$ and 4.

In all of the spectra for $n=2-5$, some intense bands are observed at 3200–3300 cm^{-1}. This small size dependency suggests that these are NH stretch vibrations of NH_3 molecules, which have a similar circumstance in the products.

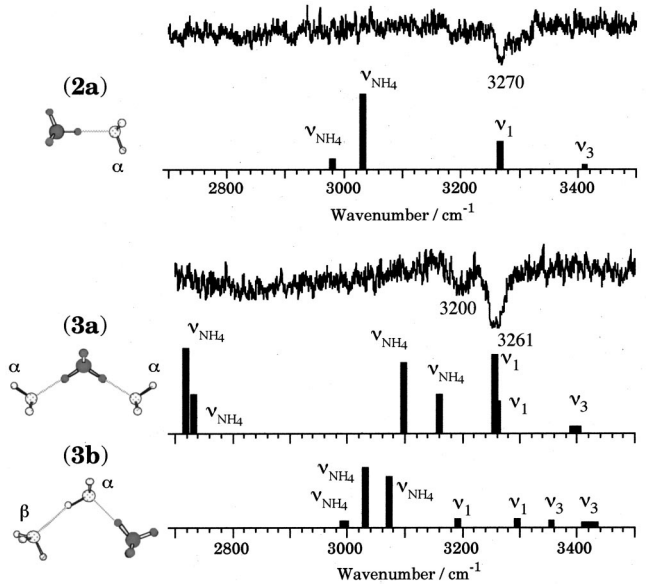

FIG. 8. Theoretical IR spectra of $(NH_3)_{n-1}NH_4$ ($n=2$ and 3) compared with the experimental ones.

The broad band below 3100 cm^{-1} may be assigned to the hydrogen-bonded NH stretches of NH_4, because the N–H bonds in NH_4 are expected to be very weak,[33,34] their stretch frequencies should be extremely low compared to those of NH_3. Band broadening may be due to a vibrational predissociation.

2. Harmonic frequencies and IR intensities for n=2 and 3

The geometries, energetics, and electronic states of $(NH_3)_{n-1}NH_4$ ($n=1-5$) were theoretically investigated at the UMP2 level with the 6-311++G(d,p) basis sets augmented by diffuse *sp* functions on N atoms in a previous study.[35] The harmonic frequencies, IR intensities and normal modes of $(NH_3)_{2,3}NH_4$, calculated at the same level, are listed in Table IV. The theoretical IR spectra against the scaled frequency are compared with the experiment in Fig. 8. The scale factor (0.942) was determined by the average ratio between the experimental fundamental and calculated harmonic frequencies of an isolated NH_3 molecule.[28]

TABLE IV. Harmonic frequencies (cm^{-1}) and IR intensities (km/mol) of NH stretches in $NH_4(NH_3)_{n-1}$ clusters at the MP2 level with the extended basis sets.

2a					3a					3b				
Expt.	Calc.	Int.	Sym.	Mode	Expt.	Calc.	Int.	Sym.	Mode	Expt.	Calc.	Int.	Sym.	Mode
	2660	15	A_1	H-bonded NH str (NH_4,v_1)		2723	1885	A_1	H-bonded NH str (NH_4,v_1)		2471	95	A	H-bonded NH str (NH_4,v_1)
						2737	806	B_2	H-bonded NH str (NH_4,v_3)		2998	57	A	non-H-bonded NH str (NH_4,v_3)
	2986	81	A_1	non-H-bonded NH str (NH_4,v_3)		3103	1542	A_1	non-H-bonded NH str (NH_4,v_3)		3037	1314	A	non-H-bonded NH str (NH_4,v_3)
	3037	1018	E	non-H-bonded NH str (NH_4,v_3)		3163	813	B_1	non-H-bonded NH str (NH_4,v_3)		3078	1115	A	non-H-bonded NH str (NH_4,v_3)
3270	3274	361	A_1	non-H-bonded NH str (α,v_1)	3261	3260	1730	B_2	non-H-bonded NH str (α,v_1)	3200	3196	94	A	H-bonded NH str (α,v_1)
						3264	691	A_1	non-H-bonded NH str (α,v_1)		3299	92	A	non-H-bonded NH str (β,v_1)
	3411	17	E	non-H-bonded NH str (α,v_3)		3400	12	A_1	non-H-bonded NH str (α,v_3)		3360	96	A	H-bonded NH str (α,v_3)
						3401	4	B_2	non-H-bonded NH str (α,v_3)		3419	16	A	non-H-bonded NH str (α,v_3)
						3402	12	B_1	non-H-bonded NH str (α,v_3)		3429	20	A	non-H-bonded NH str (β,v_3)
						3402	0	A_2	non-H-bonded NH str (α,v_3)		3437	14	A	non-H-bonded NH str (β,v_3)

The frequencies of the NH_3 vibrations were computed to be higher than those of NH_4 in both $n=2$ and 3 clusters, as one would expect. This nature is also found in larger clusters.

The calculated frequency (3274 cm^{-1}) of a non-hydrogen-bonded NH stretch of NH_3 in **2a** agrees almost perfectly with the frequency of the observed band (3270 cm^{-1}) for $n=2$. Consistently with the observation in the time-resolved spectrum for $n=3$, near-degenerate strong bands at 3260 and 3264 cm^{-1} for non-hydrogen-bonded NH stretches in the side NH_3 molecules in **3a**, and the bonded NH stretch band at 3196 cm^{-1} in **3b** correspond extremely well to the strong and weak bands observed at 3261 and 3200 cm^{-1}, respectively. These excellent agreements seem to support the tentative assignments in the preceding section.

On the other hand, the calculations predict additional strong bands derived from the NH_4 at 3037 cm^{-1} for **2a**, at 3103 and 3163 cm^{-1} for **3a**, and at 3037 and 3078 cm^{-1} for **3b** in the region where only a weak band is observed for both *n*. The sharp disagreement between the experiment and theory may result from the strong anharmonicity of the NH_4 vibrations, namely, the predissociative nature of the potential surface along the NH stretch modes in NH_4. In fact, the energy barrier of $NH_4 \rightarrow NH_3 + H$ from NH_4 was calculated to be $\sim$4700 cm^{-1} at the present level, indicating the harmonic approximation for NH stretches in NH_4 vastly overestimate the fundamental frequencies. A more elaborated analysis based on the global potential surface is necessary for a definite assignment of the spectra.

C. Discussion of the ESHT mechanism in terms of a geometrical change

In this section, we discuss the ESHT mechanism from the view point of cluster structures. For $n=2$, the geometry of the ESHT product is expected straightforwardly to be **2a** irrespective of the cyclic or open hydrogen bonds in $PhOH-(NH_3)_2$ (**IIa** and **IIb**).

For $n=3$, the REMPI spectrum indicates little geometrical change by the $S_1 \leftarrow S_0$ electronic transition; the reactant, $PhOH-(NH_3)_3$ in S_1, is most likely the cyclic form. The ESHT in this structure does not lead directly to $(NH_3)_2NH_4$, where NH_4 is located between two NH_3 molecules. Thus, the most stable isomer, **3a**, may be generated by isomerization, which is consistent with the coexistence of isomer bands in the electronic spectrum. From the optimized geometry, it is naturally expected that the second most stable isomer **3b** with the $NH_4-NH_3-NH_3$-type structure is initially generated. In other words, the reaction products have a memory of the reactant structures, which is, so to speak, a "*memory effect*."

The vibrational spectrum of the reactant together with the electronic spectrum of the product for $n=4$ shows that not only the most stable structure, but also the linear isomers of $(NH_3)_3NH_4$, are produced by the photoinduced reaction initiated at the cyclic $PhOH-(NH_3)_4$. We can also expect the *memory effect* for this size.

We have previously shown based on the electronic spectrum and theoretical calculations of the $n=5$ reaction product that the most stable structure, in which the central NH_4 is surrounded by four NH_3 molecules, is generated by the ESHT, though we cannot be conclusive about the coexistence of the isomers. The structure of the reactant (**Vc**) suggests that a geometrical change of the product, such as the migration of NH_3, occurs after, or simultaneously with, the hydrogen transfer. To investigate the *memory effect* directly in the clusters, we are now conducting picosecond time-resolved UV–IR–UV ion dip spectroscopy.

V. CONCLUSION

In the present work, we successfully measured the vibrational spectra of $PhOH-(NH_3)_n$ in S_0 and $(NH_3)_{n-1}NH_4$ $(n=2-5)$ generated by photoinduced reactions of the former clusters by UV–IR–UV ion dip spectroscopy. We also studied the structures and IR spectra by *ab initio* MO calculations at the MP2 level with large basis sets.

By combining the experiments and theoretical calculations, we have revealed the structural features of the clusters. The reactant geometries of the ESHT for $n \geqslant 3$ do not lead to direct formation of the most stable product radicals, but to the isomers indicated by the electronic absorption spectra and calculations. The structure of the products initially generated by the photoinduced reactions is considered to reflect the reactant geometries, which we call the *memory effect*.

In all vibrational spectra of the products, $(NH_3)_{n-1}NH_4$ $(n=2-5)$, strong bands are observed at 3200–3300 cm^{-1}. We have tentatively assigned these bands to the NH stretch vibrations in solvating NH_3 molecules based on their size independence and the coincidence of the frequencies with the calculations. The bands derived from the NH_4 are probably shifted to a lower region than we scanned, and are extremely broadened due to the predissociative nature of the potential surface, though a further effort beyond the harmonic approximation is necessary.

For a deeper understanding of the geometrical change during ESHT, a dynamic study with the time-resolved vibrational and electronic spectra as well as a theoretical investigation of the potential surfaces are indispensable. Such research is now in progress. The results will be presented elsewhere.

ACKNOWLEDGMENTS

This work was supported in part by a Grant-in-Aid from the Ministry of Education, Culture, Sports, Science and Technology (MEXT). A part of the computations was carried out at the Research Center for Computational Science at Okazaki National Research Institutes. The authors thank the Computer Center for the allotment of CPU time. K.H. is grateful for support by Research and Development Applying Advanced Computational Science and Technology, Japan Science and Technology Corporation (ACT–JST).

[1] D. Solgadi, C. Jouvet, and A. Tramer, J. Phys. Chem. **92**, 3313 (1988).
[2] C. Jouvet, C. Dedonder-Lardeux, M. Richard-Viard, D. Solgadi, and A. Tramer, J. Phys. Chem. **94**, 5041 (1990).
[3] J. Steadman and J. A. Syage, J. Chem. Phys. **92**, 4630 (1990).
[4] J. A. Syage, J. Soc. Photo-Opt. Instrum. Eng. **64**, 1209 (1990).
[5] J. Steadman and J. A. Syage, J. Am. Chem. Soc. **113**, 6786 (1991).
[6] J. A. Syage and J. Steadman, J. Chem. Phys. **95**, 2497 (1991).
[7] J. A. Syage and J. Steadman, J. Phys. Chem. **96**, 9606 (1992).
[8] J. A. Syage, J. Phys. Chem. **97**, 12523 (1993).

[9] O. Cheshnovsky and S. Leutwyler, J. Chem. Phys. **88**, 4127 (1988).
[10] J. J. Breen, L. W. Peng, D. M. Wilberg, A. Heikal, P. Cong, and A. Zewail, J. Chem. Phys. **92**, 805 (1990).
[11] T. Droz, R. Knochenmuss, and S. Leutwyler, J. Chem. Phys. **93**, 4520 (1990).
[12] S. K. Kim, S. Li, and E. R. Bernstein, J. Chem. Phys. **95**, 3119 (1991).
[13] E. R. Bernstein, J. Phys. Chem. **96**, 10105 (1992).
[14] M. F. Hineman, G. A. Brucker, D. F. Kelly, and E. R. Bernstein, J. Phys. Chem. **97**, 3341 (1992).
[15] M. F. Hineman, D. F. Kelly, and E. R. Bernstein, J. Chem. Phys. **99**, 4533 (1993).
[16] D. C. Lührs, R. Knochenmuss, and I. Fischer, Phys. Chem. Chem. Phys. **2**, 4335 (2000).
[17] C. Jacoby, P. Hering, M. Schmitt, W. Roth, and K. Kleinermanns, Phys. Chem. **239**, 23 (1998).
[18] M. Schmitt, C. Jacoby, M. Gerhards, C. Unterberg, W. Roth, and K. Kleinermanns, J. Chem. Phys. **113**, 2995 (2000).
[19] G. A. Pino, C. Dedonder-Lardeux, G. Grégoire, C. Jouvet, S. Martrenchard, and D. Solgadi, J. Chem. Phys. **111**, 10747 (1999).
[20] G. A. Pino, G. Grégoire, C. Dedonder-Lardeux, C. Jouvet, S. Martrenchard, and D. Solgadi, Phys. Chem. Chem. Phys. **2**, 893 (2000).
[21] G. Grégoire, C. Dedonder-Lardeux, C. Jouvet, S. Martrenchard, A. Peremans, and D. Solgadi, J. Phys. Chem. A **104**, 9087 (2000).
[22] G. Grégoire, C. Dedonder-Lardeux, C. Jouvet, S. Martrenchard, and D. Solgadi, J. Phys. Chem. A **105**, 5971 (2001).
[23] A. Iwasaki, A. Fujii, T. Watanabe, T. Ebata, and N. Mikami, J. Phys. Chem. **100**, 16053 (1996).
[24] M. J. Frisch, G. W. Trucks, H. B. Schlegel *et al.*, GAUSSIAN 98, Revision A.9, Gaussian, Inc., Pittsburgh, PA, 1998.
[25] S. Ishiuchi, M. Saeki, M. Sakai, and M. Fujii, Chem. Phys. Lett. **322**, 27 (2000).
[26] S. Martrenchard-Barra, C. Dedonder-Lardeux, C. Jouvet, D. Solgadi, M. Vervloet, G. Grégoire, and I. Dimicoli, Chem. Phys. Lett. **310**, 173 (1999).
[27] W. Siebrand, M. Z. Zgierski, Z. Smedarchina, M. Vener, and J. Kaneti, Chem. Phys. Lett. **266**, 47 (1997).
[28] G. Herzberg, *Molecular Spectra and Molecular Structure* (Van Nostrand Reinhold, New York, 1945), Vol. II.
[29] T. Watanabe, T. Ebata, S. Tanabe, and N. Mikami, J. Chem. Phys. **105**, 408 (1996).
[30] R. Yoshino, K. Hashimoto, T. Omi, S. Ishiuchi, and M. Fujii, J. Phys. Chem. A **102**, 6227 (1998).
[31] J. M. Price, M. W. Crofton, and Y. T. Lee, J. Phys. Chem. **95**, 2182 (1991).
[32] S. Ishiuchi, M. Sakai, K. Daigoku, T. Ueda, T. Yamanaka, K. Hashimoto, and M. Fujii, Chem. Phys. Lett. **347**, 87 (2001).
[33] H. Cardy, D. Liotard, A. Dargelos, F. Marinelli, and M. Roche, Chem. Phys. **123**, 73 (1988).
[34] E. Kassab and E. M. Evleth, J. Am. Chem. Soc. **109**, 1653 (1987).
[35] K. Daigoku, N. Miura, and K. Hashimoto, Chem. Phys. Lett. **346**, 81 (2001).